
Promoting Coordination through Policy Regularization in Multi-Agent Deep Reinforcement Learning

Julien Roy^{*12} Paul Barde^{*13} Félix G. Harvey¹² Derek Nowrouzezahrai¹³ Christopher Pal¹²

Abstract

In multi-agent reinforcement learning, discovering successful collective behaviors is challenging as it requires exploring a joint action space that grows exponentially with the number of agents. While the tractability of independent agent-wise exploration is appealing, this approach fails on tasks that require elaborate group strategies. We argue that coordinating the agents' policies can guide their exploration and we investigate techniques to promote such an inductive bias. We propose two policy regularization methods: TeamReg, which is based on inter-agent action predictability and CoachReg that relies on synchronized behavior selection. We evaluate each approach on four challenging continuous control tasks with sparse rewards that require varying levels of coordination. Our methodology allocates the same hyper-parameter search budget across our algorithms and baselines and we find that our approaches are more robust to hyper-parameter variations. Our experiments show that our methods significantly improve performance on cooperative multi-agent problems and scale well when the number of agents is increased. Finally, we quantitatively analyze the effects of our proposed methods on the policies that our agents learn and we show that our methods successfully enforce the qualities that we propose as proxies for coordinated behaviors.

years (Hernandez-Leal et al., 2018). A popular framework for MARL is the use of a Centralized Training and a Decentralized Execution (CTDE) procedure (Lowe et al., 2017; Foerster et al., 2018; Iqbal & Sha, 2019; Foerster et al., 2019; Rashid et al., 2018). Typically, one leverages centralized critics to approximate the value function of the aggregated observations-actions pairs and train actors restricted to the observation of a single agent. Such critics, if exposed to coordinated joint actions leading to high returns, can steer the agents' policies toward these highly rewarding behaviors. However, these approaches depend on the agents luckily stumbling on these collective actions in order to grasp their benefit. Thus, it might fail in scenarios where such behaviors are unlikely to occur by chance. We hypothesize that in such scenarios, coordination-promoting inductive biases on the policy search could help discover successful behaviors more efficiently and supersede task-specific reward shaping and curriculum learning. We support this proposition by presenting a simple and scalable environment on which agents that learn in hand-crafted coordinated policy spaces succeed remarkably faster notwithstanding the simplicity of the task.

For more realistic tasks in which coordinated strategies cannot be easily engineered and must be learned, we propose to transpose this insight by relying on two coordination proxies to bias the policy search. The first avenue, TeamReg, assumes that an agent must be able to predict the behavior of its teammates in order to coordinate with them. The second, CoachReg, supposes that coordinated agents collectively recognize different situations and synchronously switch to different sub-policies to react to them. In the following sections, we show how to derive practical policy regularizing terms from these premises and meticulously evaluate them¹.

Our contributions are threefold. Firstly, we show that coordination can crucially accelerate multi-agent learning for cooperative tasks. Secondly, we propose two novel approaches that aim at promoting such coordination through inductive biases in the policy search. Our methods augment CTDE MARL algorithms through additional multi-agent objectives that act as policy regularizers and are op-

1. Introduction

Multi-Agent Reinforcement Learning (MARL) refers to the task of training an agent to maximize its expected return by interacting with an environment that contains other learning agents. It represents a challenging branch of Reinforcement Learning (RL) with interesting developments in recent

^{*}Equal contribution ¹Mila ²Polytechnique Montréal ³McGill University. Correspondence to: Julien Roy <julien-2.roy@polymtl.ca>, Paul Barde <paul.barde@mail.mcgill.ca>.

¹Source code for the algorithms and environments will be made public upon publication of this work.

timized jointly with the main return-maximization objective. Thirdly, we design two new sparse-reward cooperative tasks in the multi-agent particle environment (Mordatch & Abbeel, 2018). We use them along with two standard multi-agent tasks to present a detailed evaluation of our approaches against three different baselines. We validate our methods’ key components by performing an ablation study and a detailed analysis of their effect on agents’ behaviors. Our experiments suggest that our TeamReg objective provides a dense learning signal that helps to guide the policy towards coordination in the absence of external reward, eventually leading it to the discovery of high performing team strategies in a number of cooperative tasks. Similarly, by enforcing synchronous sub-policy selections, CoachReg enables cooperating agents to concurrently fine-tune sub-behaviors for each collectively recognized situation yielding significant improvements on the overall performance.

2. Background

2.1. Markov Games

We consider the framework of Markov Games (Littman, 1994), a multi-agent extension of Markov Decision Processes (MDPs). A Markov Game of N independent agents is defined by the tuple $\langle \mathcal{S}, \mathcal{T}, \mathcal{P}, \{\mathcal{O}^i, \mathcal{A}^i, \mathcal{R}^i\}_{i=1}^N \rangle$ where \mathcal{S} , \mathcal{T} , and \mathcal{P} are respectively the set of all possible states, the transition function and the initial state distribution. While these are global properties of the environment, \mathcal{O}^i , \mathcal{A}^i and \mathcal{R}^i are individually defined for each agent i . They are respectively the observation functions, the sets of all possible actions and the reward functions. At each time-step t , the global state of the environment is given by $s_t \in \mathcal{S}$ and every agent’s individual action vector is denoted by $a_t^i \in \mathcal{A}^i$. To select their action, each agent i only has access to its own observation vector o_t^i which is extracted by the observation function \mathcal{O}^i from the global state s_t . The initial state s_0 is sampled from the initial state distribution $\mathcal{P} : \mathcal{S} \rightarrow [0, 1]$ and the next state s_{t+1} is sampled from the probability distribution over the possible next states given by the transition function $\mathcal{T} : \mathcal{S} \times \mathcal{S} \times \mathcal{A}^1 \times \dots \times \mathcal{A}^N \rightarrow [0, 1]$. Finally, at each time-step, each agent receives an individual scalar reward r_t^i from its reward function $\mathcal{R}^i : \mathcal{S} \times \mathcal{S} \times \mathcal{A}^1 \times \dots \times \mathcal{A}^N \rightarrow \mathbb{R}$. Agents aim at maximizing their expected discounted return $\mathbb{E} \left[\sum_{t=0}^T \gamma^t r_t^i \right]$ over the time horizon T , where $\gamma \in [0, 1]$ is a discount factor.

2.2. Multi-Agent Deep Deterministic Policy Gradient

MADDPG (Lowe et al., 2017) is an adaptation of the Deep Deterministic Policy Gradient algorithm (Lillicrap et al., 2015) to the multi-agent setting. It allows the training of cooperating and competing decentralized policies through the use of a centralized training procedure. In this

framework, each agent i possesses its own deterministic policy μ^i for action selection and critic Q^i for state-action value estimation, which are respectively parametrized by θ^i and ϕ^i . All parametric models are trained off-policy from previous transitions $\zeta_t := (\mathbf{o}_t, \mathbf{a}_t, \mathbf{r}_t, \mathbf{o}_{t+1})$ uniformly sampled from a replay buffer \mathcal{D} . Note that $\mathbf{o}_t := [o_t^1, \dots, o_t^N]$ is the joint observation vector and $\mathbf{a}_t := [a_t^1, \dots, a_t^N]$ is the joint action vector, obtained by concatenating the individual observation vectors o_t^i and action vectors a_t^i of all N agents. Each centralized critic is trained to estimate the expected return for a particular agent i from the Q-learning loss (Watkins & Dayan, 1992):

$$\mathcal{L}^i(\phi^i) = \mathbb{E}_{\zeta_t \sim \mathcal{D}} \left[\frac{1}{2} (Q^i(\mathbf{o}_t, \mathbf{a}_t; \phi^i) - y_t^i)^2 \right] \quad (1)$$

$$y_t^i = r_t^i + \gamma Q^i(\mathbf{o}_{t+1}, \mathbf{a}_{t+1}; \bar{\phi}^i) \Big|_{a_{t+1}^j = \mu^j(o_{t+1}^j; \bar{\theta}^j) \forall j}$$

For a given set of weights w , we define its target counterpart \bar{w} , updated from $\bar{w} \leftarrow \tau w + (1 - \tau)\bar{w}$ where τ is a hyper-parameter. Each policy is updated to maximize the expected discounted return of the corresponding agent i :

$$J_{PG}^i(\theta^i) = \mathbb{E}_{\mathbf{o}_t \sim \mathcal{D}} \left[Q^i(\mathbf{o}_t, \mathbf{a}_t) \Big|_{\substack{a_t^i = \mu^i(o_t^i; \theta^i), \\ a_t^j = \mu^j(o_t^j; \bar{\theta}^j) \forall j \neq i}} \right] \quad (2)$$

By taking into account *all* agents’ observation-action pairs when guiding an agent’s policy, the value-functions are trained in a centralized, stationary environment, despite taking place in a multi-agent setting. In addition, this mechanism can allow to implicitly learn coordinated strategies that can then be deployed in a decentralized way. However, this procedure does not encourage the *discovery* of coordinated strategies since high-reward behaviors have to be randomly experienced through unguided exploration.

3. Motivation

In this section, we aim to answer the following question: can coordination help the discovery of effective policies in cooperative tasks? Intuitively, coordination can be defined as an agent’s behavior being informed by the behavior of another agent, i.e. structure in the agents’ interactions. Namely, a team where agents act independently of one another would not be coordinated.

We consider a very simple Markov Game consisting of a chain leading to a termination state as depicted in Figure 1. At each time-step, both agents receive $r_t = -1$. The joint action of these two agents in this environment is given by $\mathbf{a} \in \mathcal{A} = \mathcal{A}^1 \times \mathcal{A}^2$, where $\mathcal{A}^1 = \mathcal{A}^2 = \{0, 1\}$. Agent i tries to go right when selecting $a^i = 0$ and left when selecting $a^i = 1$. However, to transition to a different state both agents need to perform the same action at the same time (two lefts or two rights).

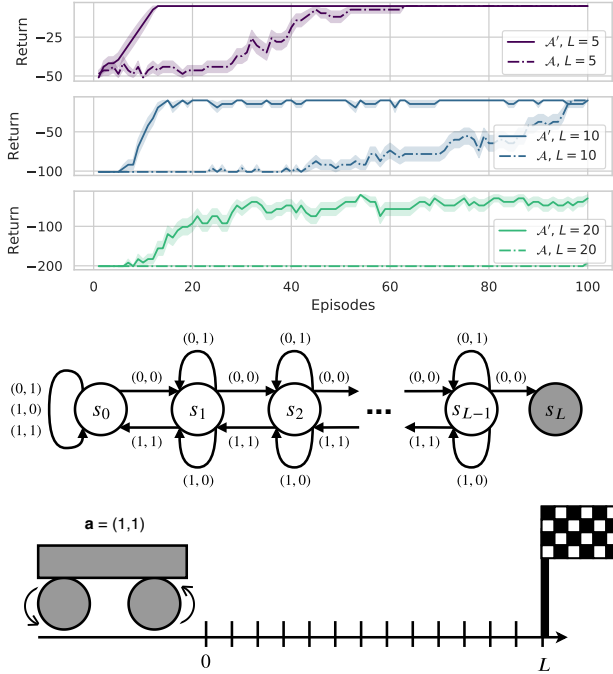


Figure 1: (Top) The tabular Q-learning agents learn much more efficiently when constrained to the space of coordinated policies (solid lines) than in the original action space (dashed lines). (Bottom) Simple Markov Game consisting of a chain leading to a terminal state (in grey). Agents can be seen as the two wheels of a vehicle so that their actions need to be in agreement for the vehicle to move. The detailed experimental setup is reported in Appendix A.

Let us now consider a slight variant of this environment with a different joint action structure $\mathcal{A}' \in \mathcal{A}'$ for which the action of the second agent has been modified so that:

$$\mathbf{a}' = \begin{pmatrix} a^{1'} = a^1 \\ a^{2'} = a^1 a^2 + (1 - a^1)(1 - a^2) \end{pmatrix}, \begin{pmatrix} a^1 \\ a^2 \end{pmatrix} \in \mathcal{A}$$

The second agent still learns a state-action value function $Q^2(s, a^2)$ with $a^2 \in \mathcal{A}^2$, but is now augmented with a hard-coded coordination module. This module maps (a^1, a^2) to $a^{2'}$ in such a way that the primitive action a^2 effectively determines whether the second agent acts in *agreement* or in *disagreement* with the first agent. In other words, if $a^2 = 1$, then $a^{2'} = a^1$ (agreement) and if $a^2 = 0$, then $a^{2'} = 1 - a^1$ (disagreement). This yields coordination in the sense that it is possible to predict the first action $a^{1'}$ by observing the second action $a^{2'}$ and either one of the two primitive actions a^1 or a^2 . Mathematically, there exists two functions f_1 and f_2 , such that $a^{1'} = f_1(a^{2'}, a^1) = f_2(a^{2'}, a^2)$. For this modified setup, it can be shown that $f_1(a^{2'}, a^1) = a^1$ and $f_2(a^{2'}, a^2) = a^{2'} a^2 + (1 - a^{2'})(1 - a^2)$. In contrast, in the first setup since the mapping from \mathbf{a} to \mathbf{a}' is the identity,

we have $(a^1, a^2) = (a^{1'}, a^{2'})$ and $f_2(a^{2'}, a^2)$ cannot exist².

We train online tabular Q-learning agents on these two environments (Figure 1) and find that learning is much more efficient on the task with a constraint enforcing coordination. By design, this example uses a hard-coded mapping in order to demonstrate the effectiveness of exploring in the space of coordinated policies rather than in the unconstrained policy space. Now, the following question remains: how can one softly learn the same type of constraint throughout training for any multi-agent cooperative tasks? In the following sections, we present two algorithms that tackle this problem.

4. Coordination and Policy regularization

4.1. Team regularization

The structure present between coordinated policies can be leveraged to attain a certain degree of predictability of one agent's behavior with respect to its teammate(s). We hypothesize that the reciprocal also holds i.e. that promoting agents' predictability could foster such team structure and lead to more coordinated behaviors. This assumption is cast into the decentralized framework by training agents to predict their teammates' actions given only their own observation. For continuous control, the loss is the Mean Squared Error (MSE) between the predicted and true actions of the teammates, yielding a teammate-modelling secondary objective. While estimating teammates' policies can be used to enrich the learned representations, we further extend this objective to also drive the teammates' behaviors towards the predictions by leveraging a differentiable action selection mechanism. We call *team-spirit* this novel objective $J_{TS}^{i,j}$ between agents i and j :

$$J_{TS}^{i,j}(\theta^i, \theta^j) = -\mathbb{E}_{\mathbf{o}_t \sim \mathcal{D}} \left[\frac{1}{2} \sum_{k=1}^{|\mathcal{A}^j|} (\hat{a}_{t,k}^{i,j} - a_{t,k}^j)^2 \middle| \begin{matrix} a_t^j = \mu^j(o_t^j; \theta^j) \\ \hat{a}_t^{i,j} = \hat{\mu}^{i,j}(o_t^i; \theta^i) \end{matrix} \right] \quad (3)$$

where $\hat{\mu}^{i,j}$ is the policy head of agent i trying to predict the action of agent j . The total loss for a given agent i becomes:

$$J_{total}^i(\theta^i) = J_{PG}^i(\theta^i) + \lambda_1 \sum_j J_{TS}^{i,j}(\theta^i, \theta^j) + \lambda_2 \sum_j J_{TS}^{j,i}(\theta^j, \theta^i) \quad (4)$$

where λ_1 and λ_2 are hyper-parameters that respectively weigh how well an agent should predict its teammates' actions, and how predictable an agent should be for its teammates. We call TeamReg this dual regularization from team-spirit objectives. Figure 2 summarizes these interactions.

² This is shown in details in Appendix A

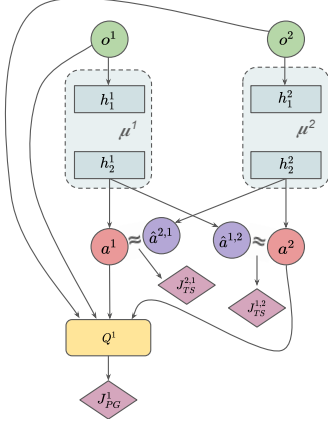


Figure 2: Illustration of TeamReg with two agents. Each agent’s policy is equipped with additional heads that are trained to predict other agents’ actions and every agent is regularized to produce actions that its teammates correctly predict. Note that the method is depicted for agent 1 only to avoid cluttering.

4.2. Coach regularization

In order to foster coordinated interactions, this method aims at teaching the agents to recognize different situations and synchronously select corresponding sub-behaviors.

4.2.1. SUB-POLICY SELECTION

Firstly, to enable explicit sub-behavior selection, we propose *policy masks* that modulate the agents’ policy. A policy mask u^j is a one-hot vector of size K with its j^{th} component set to one. In practice, we use policy masks to perform dropout (Srivastava et al., 2014) in a structured manner on $\tilde{h}_1 \in \mathbb{R}^M$, the pre-activations of the first hidden layer h_1 of the policy network π . To do so, we construct the vector u^j , which is the concatenation of C copies of u^j , in order to reach the dimensionality $M = C * K$. The element-wise product $u^j \odot \tilde{h}_1$ is then performed and only the units of \tilde{h}_1 at indices m modulo $K = j$ are kept for $m = 0, \dots, M-1$. In our contribution, each agent i generates e_t^i , its own policy mask from its observation o_t^i , to modulate its policy network. Here, a simple linear layer l^i is used to produce a categorical probability distribution $p^i(e_t^i | o_t^i)$ from which the one-hot vector is sampled:

$$p^i(e_t^i = u^j | o_t^i) = \frac{\exp(l^i(o_t^i; \theta^i)_j)}{\sum_{k=0}^{K-1} \exp(l^i(o_t^i; \theta^i)_k)} \quad (5)$$

Although the policy masking mechanism enables the agent to swiftly switch between sub-policies it does not encourage the agents to synchronously modulate their behavior.

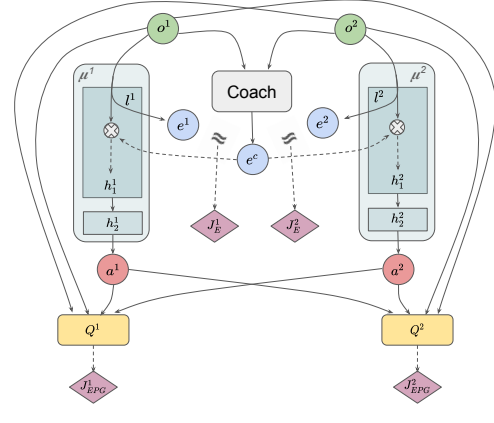


Figure 3: Illustration of CoachReg with two agents. A central model, the coach, takes all agents’ observations as input and outputs the current mode (policy mask). Agents are regularized to predict the same mask from their local observations only and optimize the corresponding sub-policy.

4.2.2. SYNCHRONOUS SUB-POLICY SELECTION

To promote synchronicity we introduce the *coach* entity, parametrized by ψ , which learns to produce policy-masks e_t^c from the joint observations, i.e. $p^c(e_t^c | \mathbf{o}_t; \psi)$. The coach is used at training time only and drives the agents toward synchronously selecting the same behavior mask. In other words, the coach is trained to output masks that (1) yield high returns when used by the agents and (2) are predictable by the agents. Similarly, each agent is regularized so that (1) its private mask matches the coach’s mask and (2) it derives efficient behavior when using the coach’s mask. At evaluation time, the coach is removed and the agents only rely on their own policy masks. The policy gradient loss when agent i is provided with the coach’s mask is given by:

$$J_{EPG}^i(\theta^i, \psi) = \mathbb{E}_{\mathbf{o}_t, \mathbf{a}_t \sim \mathcal{D}} \left[Q^i(\mathbf{o}_t, \mathbf{a}_t) \middle| \substack{a_t = \mu(o_t^i, e_t^i; \theta^i) \\ e_t^i \sim p^c(\cdot | \mathbf{o}_t; \psi)} \right] \quad (6)$$

The difference between the mask of agent i and the coach’s one is measured from the Kullback–Leibler divergence:

$$J_E^i(\theta^i, \psi) = \mathbb{E}_{\mathbf{o}_t \sim \mathcal{D}} [\text{D}_{\text{KL}}(p^c(\cdot | \mathbf{o}_t; \psi) || p^i(\cdot | o_t^i; \theta^i))] \quad (7)$$

The total loss for agent i is:

$$J_{total}^i(\theta^i) = J_{PG}^i(\theta^i) + \lambda_1 J_E^i(\theta^i, \psi) + \lambda_2 J_{EPG}^i(\theta^i, \psi) \quad (8)$$

with λ_1 and λ_2 the regularization coefficients. Similarly, the coach is trained with the following dual objective, weighted by the λ_3 coefficient:

$$J_{total}^c(\psi) = \frac{1}{N} \sum_{i=1}^N (J_{EPG}^i(\theta^i, \psi) + \lambda_3 J_E^i(\theta^i, \psi)) \quad (9)$$

In order to propagate gradients through the sampled policy mask we reparameterized the categorical distribution using the Gumbel-softmax trick (Jang et al., 2017) with a temperature of 1. We call this coordinated sub-policy selection regularization CoachReg and illustrate it in Figure 3.

Pseudocodes of our implementations are provided in Appendix D (see Algorithms 1 and 2).

5. Related Work

Many works in MARL consider explicit communication channels between the agents and distinguish between communicative actions (e.g. broadcasting a given message) and physical actions (e.g. moving in a given direction) (Foerster et al., 2016; Mordatch & Abbeel, 2018; Lazaridou et al., 2016). Consequently, they often focus on the emergence of language, considering tasks where the agents must discover a common communication protocol to succeed. Deriving a successful communication protocol can already be seen as coordination in the communicative action space and can enable, to some extent, successful coordination in the physical action space (Ahilan & Dayan, 2019). Yet, explicit communication is not a necessary condition for coordination as agents can rely on physical communication (Mordatch & Abbeel, 2018; Gupta et al., 2017).

Approaches to shape RL agents’ behaviors with respect to other agents have also been explored. Strouse et al. (2018) use the mutual information between the agent’s policy and a goal-independent policy to shape the agent’s behavior towards hiding or spelling out its current goal. However, this approach is only applicable for tasks with an explicit goal representation and is not specifically intended for coordination. Jaques et al. (2019) approximate the direct causal effect between agent’s actions and use it as an intrinsic reward to encourage social empowerment. This approximation relies on each agent learning a model of other agents’ policies to predict its effect on them. In general, this type of behavior prediction can be referred to as *agent modelling* (or *opponent modelling*) and has been used in previous work to enrich representations when amongst stationary non-learning teammates (Hernandez-Leal et al., 2019), to stabilise the learning dynamics (He et al., 2016) or to classify the opponent’s play style (Schadd et al., 2007).

Finally, Barton et al. (2018) propose convergent cross mapping (CCM) to measure the degree of effective coordination between two agents. Although this may represent an interesting avenue for behavior analysis, it fails to provide a tool for effectively enforcing coordination as CCM must be computed over long time series which makes it an impractical learning signal for single-step temporal difference methods.

To our knowledge, this work is the first to extend agent modelling to derive a novel inductive bias towards team-

predictable policies and to introduce a collective, agent induced, modulation of the policies without an explicit communication channel. These coordination proxies are enforced throughout training only which allows to carry the learned coordinated behaviors at test time, when all agents act in a decentralized fashion.

6. Training environments

All of our tasks are based on the OpenAI multi-agent particle environments (Mordatch & Abbeel, 2018). SPREAD and CHASE were introduced by (Lowe et al., 2017). We use SPREAD as is but with sparse rewards. CHASE is modified with a prey controlled by repulsion forces so that only the predators are learnable, as we wish to focus on coordination in cooperative tasks. Finally we introduce COMPROMISE and BOUNCE where agents are physically tied together. While non-zero return can be achieved in these tasks by selfish agents, they all benefit from coordinated strategies and optimal return can only be achieved by agents working closely together. Figure 4 presents a visualization and a brief description for all four tasks. In all tasks, agents receive as observation their own global position and velocity as well as the relative position of other entities. A more detailed description is provided in Appendix B. Note that work showcasing experiments on these environments often use discrete action spaces and dense rewards (e.g. the proximity with the objective) (Iqbal & Sha, 2019; Lowe et al., 2017; Jiang & Lu, 2018). In our experiments, agents learn with continuous action spaces and from sparse rewards.

7. Results and Discussion

The proposed methods offer a way to incorporate new inductive biases in CTDE multi-agent policy search algorithms. We evaluate them by extending MADDPG, a state of the art algorithm widely used in the MARL literature. We compare against vanilla MADDPG as well as two of its variants in the four cooperative multi-agent tasks described in Section 6. The first variant (DDPG) is the single-agent counterpart of MADDPG (decentralized training). The second (MADDPG + sharing) shares the policy and value-function models across agents. Additionally to the two proposed algorithms and the three baselines, we present results for two ablated versions of our methods. The first ablation (MADDPG + agent modelling) is similar to TeamReg but with $\lambda_2 = 0$, which results in only enforcing agent modelling and not encouraging agent predictability. The second ablation (MADDPG + policy mask) uses the same policy architecture as CoachReg, but with $\lambda_{1,2,3} = 0$, which means that agents still predict and apply a mask to their own policy, but synchronicity is not encouraged.

To offer a fair comparison between all methods, the hyper-

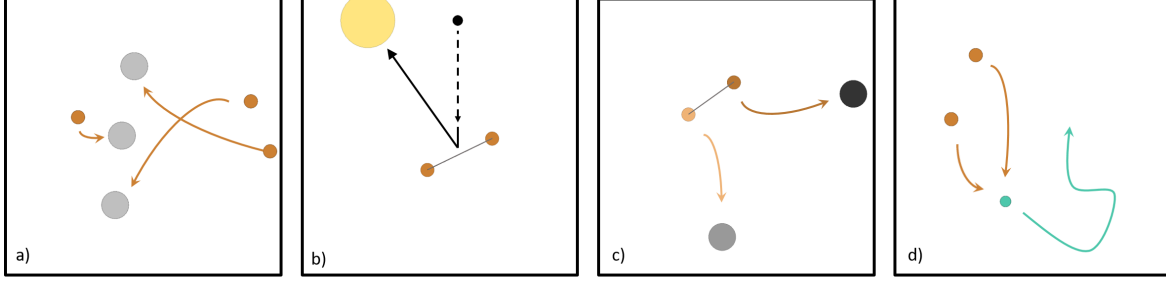


Figure 4: Multi-agent tasks we employ. (a) SPREAD: Agents must spread out and cover a set of landmarks. (b) BOUNCE: Two agents are linked together by a spring and must position themselves so that the falling black ball bounces towards a target. (c) COMPROMISE: Two linked agents must compete or cooperate to reach their own assigned landmark. (d) CHASE: Two agents chase a (non-learning) prey (turquoise) that moves w.r.t repulsion forces from predators and walls.

parameter search routine is the same for each algorithm and environment (see Appendix E.1). For each search-experiment (one per algorithm per environment), 50 randomly sampled hyper-parameter configurations each using 3 training seeds (total of 150 runs) are used to train the models for 15,000 episodes. For each algorithm-environment pair, we then select the best hyper-parameter configuration for the final comparison and retrain them on 10 seeds for twice as long. We give all details about the training setup and model selection in Appendix C and E.2. The results of the hyper-parameter searches are given in Appendix E.5 where Figure 9 shows that our proposed coordination regularizers can improve robustness to hyper-parameters despite the fact that they have more hyper-parameters to search over.

7.1. Asymptotic Performance

Figure 5 reports the average learning curves. We observe that CoachReg significantly improves performance on three environments (SPREAD, BOUNCE and COMPROMISE). The same can be said for TeamReg except for COMPROMISE, the only task with an adversarial component, where it significantly underperforms compared to the other algorithms. We discuss this specific case in Section 7.2. All algorithms perform similarly well on CHASE, with a slight advantage to the one using parameter sharing, yet this superiority is restricted to this task where the optimal play is to move symmetrically and squeeze the prey into a corner.

Regarding the ablated versions of our methods, the use of unsynchronized policy masks might result in swift and unpredictable behavioral changes and make it difficult for agents to perform together and coordinate. Experimentally, “MADDPG + policy mask” performs similarly or worse than MADDPG on all but one environment, and never outperforms the full CoachReg approach. However, policy masks alone seem sufficient to succeed on SPREAD, which is about selecting a landmark from a set. Finally “MADDPG + agent modelling” does not drastically improve

on MADDPG apart from on the SPREAD environment, and is always outperformed by the full TeamReg except on the COMPROMISE task, which we discuss in Section 7.2.

7.2. Effects of enforcing predictable behavior

First, we investigate the reason for TeamReg’s poor performance on COMPROMISE. Then, we analyse how TeamReg might be helpful in other environments.

COMPROMISE is the only task with a competitive component (i.e. the only one in which agents do not share their rewards). The two agents being strapped together, a good policy has both agents reach their landmark successively (e.g. by having both agents navigate towards the closest landmark). However, if one agent never reaches for its landmark, the optimal strategy for the other one becomes to drag it around and always go for its own, leading to a strong imbalance in the return cumulated by both agents. While such scenario doesn’t occur for the other algorithms, we found TeamReg to often lead to such domination cases (see Figure 10 in Appendix F). Figure 6 depicts the agents’ performance difference for every 150 runs of the hyperparameter search for TeamReg and the baselines, and shows that (1) TeamReg is the only algorithm that does lead to large imbalances in performance between the two agents and (2) that these cases where one agent becomes dominant are all associated with high values of λ_2 , which drives the agents to behave in a predictable fashion to one another. However, the dominated agent eventually gets exposed more and more to sparse reward gathered by being dragged (by chance) onto its own landmark, picks up the goal of the task and starts pulling in its own direction, which causes the average return over agents to drop as we see happening midway during training in Figure 5. This experiment suggests that using a predictability-based team-regularization in a competitive task can be harmful; quite understandably, you might not want to optimize an objective that aims at making your behavior predictable to your opponent.

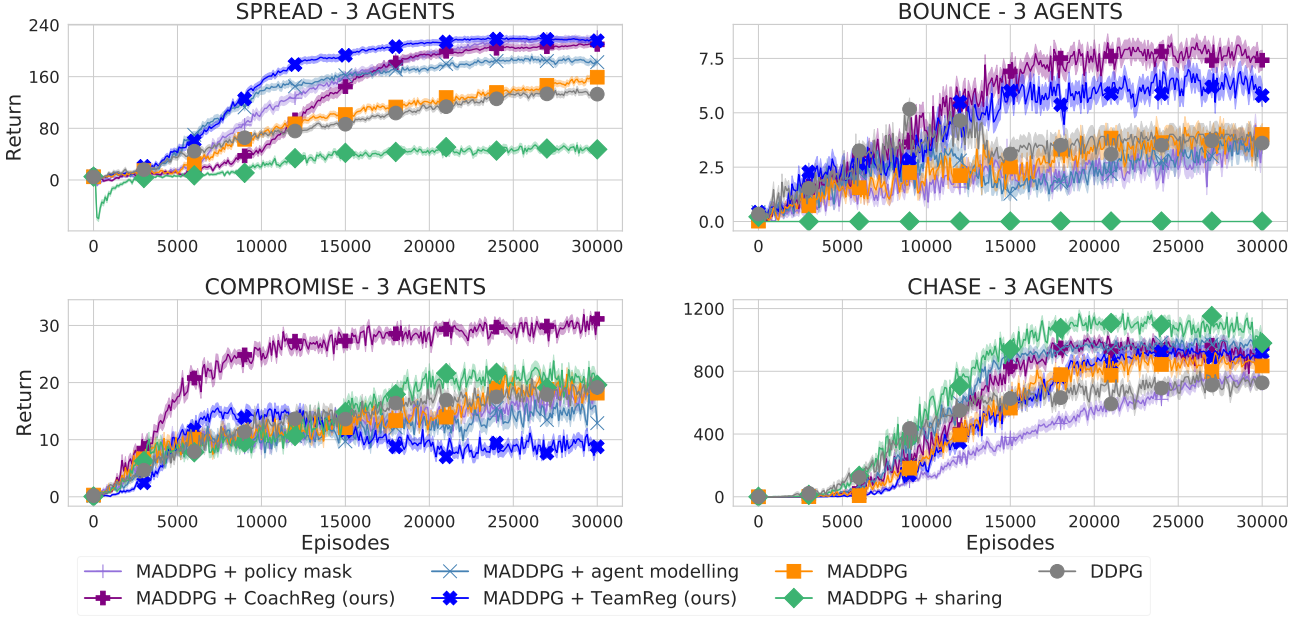


Figure 5: Learning curves (mean return over agents) for our two proposed algorithms, two ablations and three baselines on all four environments. Solid lines are the mean and envelopes are the Standard Error (SE) across the 10 training seeds.

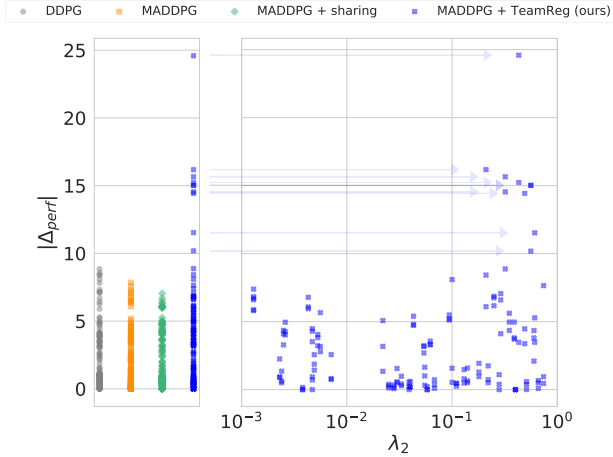


Figure 6: Average performance difference (Δ_{perf}) between the two agents in COMPROMISE for each 150 runs of the hyper-parameter searches (left). All occurrences of abnormally high performance difference are associated with high values of λ_2 (right).

Now, on SPREAD and BOUNCE, TeamReg significantly improves the performance over the baselines. We aim to analyze here the effects of λ_2 on cooperative tasks and investigate if it does make the agent modelling task more successful (by encouraging agents to be predictable). To this end, we compare, on the SPREAD environment, the team-spirit losses between TeamReg and its ablated versions. The curves of the team-spirit loss (defined in Section 4.1)

which measures the prediction error when agents try to predict their teammates’ actions are presented in Figure 7. Initially, due to the weight initialization, the predicted and actual actions both have relatively small norms yielding small values of team-spirit loss. As training goes on (~ 1000 episodes), the norms of the action-vector increase and the regularization loss becomes more important. As expected, MADDPG leads to the highest team-spirit loss as it is not trained to predict the actions of other agents correctly. When using only the agent-modelling objective ($\lambda_1 > 0$), the agents significantly decrease the team-spirit loss, but it never reaches values as low as when using the full TeamReg objective. Finally, when also pushing agents to be predictable ($\lambda_2 > 0$), the agents best predict each others’ actions and performance is also improved. We also notice that the team-spirit loss increases when performance starts to improve i.e. when agents start to master the task (~ 8000 episodes). Indeed, once the reward maximisation signals becomes stronger, the relative importance of the auxiliary objective is reduced. We hypothesize that being predictable with respect to one-another may push agents to explore in a more structured and informed manner in the absence of reward signal, as similarly pursued by intrinsic motivation approaches (Chentanez et al., 2005).

7.3. Analysis of synchronous sub-policy selection

In this section we aim at experimentally verifying that CoachReg yields the desired behavior: agents *synchronously* alternating between *varied* sub-policies. A special attention

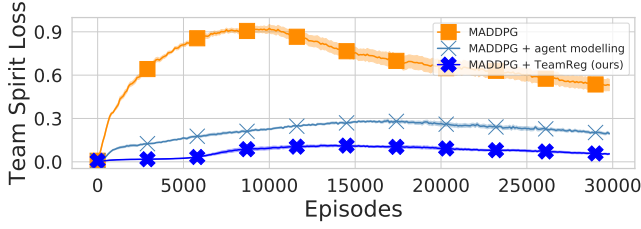


Figure 7: Effect of enabling and disabling the regularizing coefficients λ_1 and λ_2 on the ability of agents to predict their teammates behavior. Solid lines and envelope are average and standard error over 10 seeds on SPREAD.

is given when the sub-policies are interpretable. To this end we record and analyze the agents’ policy masks on 100 different episodes for each task.

From the collected masks, we reconstructed the empirical mask distribution of each agent (see Figure 11 in Appendix G.1) whose entropy provides an indication of the mask diversity used by a given agent. Figure 8 (left) shows the mean entropy for each environment compared to the entropy of Categorical Uniform Distributions of size k (k -CUD). It shows that, on all the environments, agents use at least two distinct masks by having non-zero entropy. In addition, agents tend to alternate between masks with more variety (close to uniformly switching between 3 masks) on SPREAD (where there are 3 agents and 3 goals) than on the other environments (comprised of 2 agents).

To test if agents are synchronously selecting the same policy mask at test time (without a coach), we compute the Hamming proximity between the agents’ mask sequences with $1 - D_h$ where D_h is the Hamming distance, i.e. the number of timesteps where the two sequences are different divided by the total number of timesteps. From Figure 8 (right) we observe that agents are producing similar mask sequences meaning that they often use the same masks at the same moments. Notably, their mask sequences are significantly more similar than the ones of two agent randomly choosing between two masks at each timestep. Finally, we observe that some settings result in the agents coming up with interesting strategies, like the one depicted in Figure 12 in Appendix G.1 where the agents alternate between two sub-policies depending on the position of the target³. These results indicate that, in addition to improving the performance on collaborative tasks, CoachReg indeed yields the expected behavior. An interesting following work would be to use entropy regularization to increase the mask usage variety and mutual information to further disentangle sub-policies.

³ Animated gifs displaying behaviors relying on synchronous sub-policy selection can be visualised at <https://sites.google.com/view/marl-coordination/>

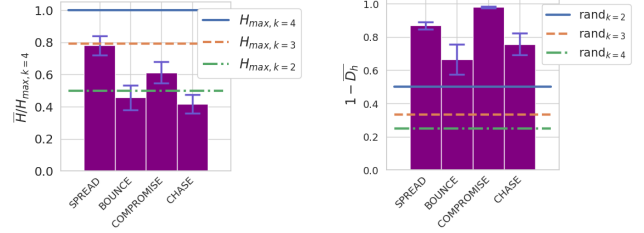


Figure 8: (Left) Entropy of the policy mask distributions for each task, averaged over agents and training seeds. $H_{max,k}$ is the entropy of a k -CUD. (Right) Hamming Proximity between the policy mask sequence of each agent averaged across agent pairs and seeds. $rand_k$ stands for agents independently sampling their masks from k -CUD. Error bars represent the standard error across seeds.

7.4. Scalability with the number of agents

To assess how the proposed methods scale to greater number of agents, we increase the number of agents in the SPREAD task from three to six agents. The results presented in Figure 15 (Appendix H.2) show that the performance benefits provided by our methods hold when the number of agents is increased. Strikingly, we also note how quickly learning becomes more challenging when the number of agents rises. Indeed, with each new agent, the coordination problem becomes more and more difficult, and that might explain why our methods that promote coordination maintain a higher degree of performance. Nonetheless, in the sparse reward setting, the complexity of the task soon becomes too difficult and none of the algorithms is able to solve it with six agents.

8. Conclusion

After showing how crucial coordination can be for multi-agent learning we proposed two policy regularization methods to promote multi-agent coordination within the CTDE framework: TeamReg, which extends inter-agent modelling to bias the policy search towards predictability and CoachReg that enforces collective and synchronized sub-policy selection. A thorough empirical evaluation of these methods showed that they significantly improve multi-agent learning on cooperative tasks. Interesting avenues for future work would be to study the proposed regularizations on other policy search methods as well as to combine both incentives and investigate how the two coordinating objectives interact. Finally, a limitation of the current formulation is that it relies on single-step metrics, which simplifies off-policy learning but also limits the longer-term coordination opportunities. A promising direction is thus to explore model-based planning approaches to promote long-term multi-agent interactions.

ACKNOWLEDGMENTS

We wish to thank Olivier Delalleau for providing insightful feedback and comments. We would also like to thank *Fonds de Recherche Nature et Technologies (FRQNT)*, Ubisoft Montréal and Mitacs for providing funding for this work as well as Compute Canada for providing the computing resources.

References

- Ahilan, S. and Dayan, P. Feudal multi-agent hierarchies for cooperative reinforcement learning. *arXiv preprint arXiv:1901.08492*, 2019.
- Ba, J. L., Kiros, J. R., and Hinton, G. E. Layer normalization. *arXiv preprint arXiv:1607.06450*, 2016.
- Barton, S. L., Waytowich, N. R., Zaroukian, E., and Asher, D. E. Measuring collaborative emergent behavior in multi-agent reinforcement learning. In *International Conference on Human Systems Engineering and Design: Future Trends and Applications*, pp. 422–427. Springer, 2018.
- Chentanez, N., Barto, A. G., and Singh, S. P. Intrinsically motivated reinforcement learning. In *Advances in neural information processing systems*, pp. 1281–1288, 2005.
- Foerster, J., Assael, I. A., de Freitas, N., and Whiteson, S. Learning to communicate with deep multi-agent reinforcement learning. In *Advances in Neural Information Processing Systems*, pp. 2137–2145, 2016.
- Foerster, J., Song, F., Hughes, E., Burch, N., Dunning, I., Whiteson, S., Botvinick, M., and Bowling, M. Bayesian action decoder for deep multi-agent reinforcement learning. *International Conference on Machine Learning*, 2019.
- Foerster, J. N., Farquhar, G., Afouras, T., Nardelli, N., and Whiteson, S. Counterfactual multi-agent policy gradients. In *Thirty-Second AAAI Conference on Artificial Intelligence*, 2018.
- Gupta, J. K., Egorov, M., and Kochenderfer, M. J. Co-operative multi-agent control using deep reinforcement learning. In *AAMAS Workshops*, 2017.
- He, H., Boyd-Graber, J., Kwok, K., and Daumé III, H. Opponent modeling in deep reinforcement learning. In *International Conference on Machine Learning*, pp. 1804–1813, 2016.
- Hernandez-Leal, P., Kartal, B., and Taylor, M. E. Is multi-agent deep reinforcement learning the answer or the question? a brief survey. *arXiv preprint arXiv:1810.05587*, 2018.
- Hernandez-Leal, P., Kartal, B., and Taylor, M. E. Agent Modeling as Auxiliary Task for Deep Reinforcement Learning. In *AAAI Conference on Artificial Intelligence and Interactive Digital Entertainment*, 2019.
- Iqbal, S. and Sha, F. Actor-attention-critic for multi-agent reinforcement learning. In *International Conference on Machine Learning*, pp. 2961–2970, 2019.
- Jang, E., Gu, S., and Poole, B. Categorical reparametrization with gumble-softmax. In *International Conference on Learning Representations (ICLR 2017)*. OpenReview. net, 2017.
- Jaques, N., Lazaridou, A., Hughes, E., Gulcehre, C., Ortega, P., Strouse, D., Leibo, J. Z., and De Freitas, N. Social influence as intrinsic motivation for multi-agent deep reinforcement learning. In *International Conference on Machine Learning*, pp. 3040–3049, 2019.
- Jiang, J. and Lu, Z. Learning attentional communication for multi-agent cooperation. In *Advances in Neural Information Processing Systems*, pp. 7254–7264, 2018.
- Kaelbling, L. P., Littman, M. L., and Moore, A. W. Reinforcement learning: A survey. *Journal of artificial intelligence research*, 4:237–285, 1996.
- Kingma, D. P. and Ba, J. Adam: A method for stochastic optimization. *arXiv preprint arXiv:1412.6980*, 2014.
- Lazaridou, A., Peysakhovich, A., and Baroni, M. Multi-agent cooperation and the emergence of (natural) language. *arXiv preprint arXiv:1612.07182*, 2016.
- Lillicrap, T. P., Hunt, J. J., Pritzel, A., Heess, N., Erez, T., Tassa, Y., Silver, D., and Wierstra, D. Continuous control with deep reinforcement learning. *arXiv preprint arXiv:1509.02971*, 2015.
- Littman, M. L. Markov games as a framework for multi-agent reinforcement learning. In *Machine learning proceedings 1994*, pp. 157–163. Elsevier, 1994.
- Lowe, R., Wu, Y., Tamar, A., Harb, J., Abbeel, O. P., and Mordatch, I. Multi-agent actor-critic for mixed cooperative-competitive environments. In *Advances in Neural Information Processing Systems*, pp. 6379–6390, 2017.
- Mordatch, I. and Abbeel, P. Emergence of grounded compositional language in multi-agent populations. In *Thirty-Second AAAI Conference on Artificial Intelligence*, 2018.
- Nair, V. and Hinton, G. E. Rectified linear units improve restricted boltzmann machines. In *Proceedings of the 27th international conference on machine learning (ICML-10)*, pp. 807–814, 2010.

- Rashid, T., Samvelyan, M., Witt, C. S., Farquhar, G., Foerster, J., and Whiteson, S. Qmix: Monotonic value function factorisation for deep multi-agent reinforcement learning. In *International Conference on Machine Learning*, pp. 4292–4301, 2018.
- Schadd, F., Bakkes, S., and Spronck, P. Opponent modeling in real-time strategy games. In *GAMEON*, pp. 61–70, 2007.
- Srivastava, N., Hinton, G., Krizhevsky, A., Sutskever, I., and Salakhutdinov, R. Dropout: a simple way to prevent neural networks from overfitting. *The journal of machine learning research*, 15(1):1929–1958, 2014.
- Strouse, D., Kleiman-Weiner, M., Tenenbaum, J., Botvinick, M., and Schwab, D. J. Learning to share and hide intentions using information regularization. In *Advances in Neural Information Processing Systems*, pp. 10270–10281, 2018.
- Uhlenbeck, G. E. and Ornstein, L. S. On the theory of the brownian motion. *Physical review*, 36(5):823, 1930.
- Watkins, C. J. and Dayan, P. Q-learning. *Machine learning*, 8(3-4):279–292, 1992.

A. Additional details for experiment presented in Section 3 Motivation

Proposition 1.1

If

$$a^{1'} = a^1, \forall a^1 \in \{0, 1\} \quad (10)$$

$$a^{2'} = a^1 a^2 + (1 - a^1)(1 - a^2), \forall \begin{pmatrix} a^1 \\ a^2 \end{pmatrix} \in \{0, 1\}^2 \quad (11)$$

$$f_1(a^{2'}, a^1) = a^1, \forall \begin{pmatrix} a^{2'} \\ a^1 \end{pmatrix} \in \{0, 1\}^2 \quad (12)$$

$$f_2(a^{2'}, a^2) = a^{2'} a^2 + (1 - a^{2'})(1 - a^2), \forall \begin{pmatrix} a^{2'} \\ a^2 \end{pmatrix} \in \{0, 1\}^2 \quad (13)$$

then

$$a^{1'} = f_1(a^{2'}, a^1) \quad (14)$$

$$a^{1'} = f_2(a^{2'}, a^2) \quad (15)$$

Proof. From Eq. (10) and Eq. (12) we have

$$a^{1'} = a^1 = f_1(a^{2'}, a^1) \quad (16)$$

which proves Eq. (14).

Substituting Eq. (11) in Eq. (13) and using the following identities for binary variables

$$\begin{cases} x^2 = x \\ (1 - x)^2 = (1 - x) \\ x(1 - x) = 0 \end{cases} \quad \forall x \in \{0, 1\}$$

we get

$$\begin{aligned} f_2(a^{2'}, a^2) &= a^1 a^2 + (1 - a^2) - (1 - a^1)(1 - a^2) \\ &= a^1 a^2 + (1 - a^2) a^1 \\ &= a^1 \end{aligned} \quad (17)$$

Finally, using Eq. (10) we get

$$f_2(a^{2'}, a^2) = a^{1'} \quad (18)$$

Proving Eq. (15).

Proposition 1.2

If

$$a^{1'} = a^1, \forall a^1 \in \{0, 1\} \quad (19)$$

$$a^{2'} = a^2, \forall a^2 \in \{0, 1\} \quad (20)$$

then there is no function f_2 such that

$$a^{1'} = f_2(a^{2'}, a^2) \quad (21)$$

Proof. Imagine that f_2 would exist such that Eq. (21), then using Eq. (20) we would have an function g such that:

$$a^{1'} = f_2(a^{2'}, a^2) = f_2(a^{2'}, a^{2'}) = g(a^{2'}) \quad (22)$$

which would contradict Eq. (19) and Eq. (20) where $a^{1'}$ and $a^{2'}$ are independent, therefore f_2 cannot exist.

Experimental details We trained each agent i with online Q-learning (Watkins & Dayan, 1992) on the $Q^i(a^i, s)$ table using Boltzmann exploration (Kaelbling et al., 1996). The Boltzmann temperature is fixed to 1 and we set the learning rate to 0.05 and the discount factor to 0.99. After each learning episode we evaluate the current greedy policy on 10 episodes and report the mean return. Curves are averaged over 20 seeds and the shaded area represents the standard error.

B. Tasks descriptions

SPREAD (Figure 4a): In this environment, there are 3 agents (small orange circles) and 3 landmarks (bigger gray circles). At every timestep, agents receive a team-reward $r_t = n - c$ where n is the number of landmarks occupied by at least one agent and c the number of collisions occurring at that timestep. To maximize their return, agents must therefore spread out and cover all landmarks. Initial agents’ and landmarks’ positions are random. Termination is triggered when the maximum number of timesteps is reached.

BOUNCE (Figure 4b): In this environment, two agents (small orange circles) are linked together with a spring that pulls them toward each other when stretched above its relaxation length. At episode’s mid-time a ball (smaller black circle) falls from the top of the environment. Agents must position correctly so as to have the ball bounce on the spring towards the target (bigger beige circle), which turns yellow if the ball’s bouncing trajectory passes through it. They receive a team-reward of $r_t = 0.1$ if the ball reflects towards the side walls, $r_t = 0.2$ if the ball reflects towards the top of the environment, and $r_t = 10$ if the ball reflects towards the target. At initialisation, the target’s and ball’s vertical position is fixed, their horizontal positions are random. Agents’ initial positions are also random. Termination is triggered when the ball is bounced by the agents or when the maximum number of timesteps is reached.

COMPROMISE (Figure 4c): In this environment, two agents (small orange circles) are linked together with a spring that pulls them toward each other when stretched above its relaxation length. They both have a distinct assigned landmark (light gray circle for light orange agent, dark gray circle for dark orange agent), and receive a reward of $r_t = 10$ when they reach it. Once a landmark is reached by its corresponding agent, the landmark is randomly relocated in the environment. Initial positions of agents and landmark are random. Termination is triggered when the maximum number of timesteps is reached.

CHASE (Figure 4d): In this environment, two predators (orange circles) are chasing a prey (turquoise circle). The prey moves with respect to a scripted policy consisting of repulsion forces from the walls and predators. At each timestep, the learning agents (predators) receive a team-reward of $r_t = n$ where n is the number of predators touching the prey. The prey has a greater max speed and acceleration than the predators. Therefore, to maximize their return, the two agents must coordinate in order to squeeze the prey into a corner or a wall and effectively trap it there. Termination is triggered when the maximum number of time steps is reached.

C. Training details

In all of our experiments, we use the Adam optimizer (Kingma & Ba, 2014) to perform parameter updates. All models (actors, critics and coach) are parametrized by feedforward networks containing two hidden layers of 128 units. We use the Rectified Linear Unit (ReLU) (Nair & Hinton, 2010) as activation function and layer normalization (Ba et al., 2016) on the pre-activations unit to stabilize the learning. We use a buffer-size of 10^6 entries and a batch-size of 1024. We collect 100 transitions by interacting with the environment for each learning update. For all tasks in our hyper-parameter searches, we train the agents for 15,000 episodes of 100 steps and then re-train the best configuration for each algorithm-environment pair for twice as long (30,000 episodes) to ensure full convergence for the final evaluation. The scale of the exploration noise is kept constant for the first half of the training time and then decreases linearly to 0 until the end of training. We use a discount factor γ of 0.95 and a gradient clipping threshold of 0.5 in all experiments. Finally for CoachReg, we fixed K to 4 meaning that agents could choose between 4 sub-policies. Since policies’ hidden layers are of size 128 the corresponding value for C is 32. All experiments were run on Intel E5-2683 v4 Broadwell (2.1GHz) CPUs in less than 12 hours.

D. Algorithms

Algorithm 1 Team

Randomly initialize N critic networks Q^i and actor networks μ^i
 Initialize the target weights
 Initialize one replay buffer \mathcal{D}
for episode from 0 to number of episodes **do**
 Initialize random processes \mathcal{N}^i for action exploration
 Receive initial joint observation \mathbf{o}_0
 for timestep t from 0 to episode length **do**
 Select action $a_i = \mu^i(o_t^i) + \mathcal{N}_t^i$ for each agent
 Execute joint action \mathbf{a}_t and observe joint reward \mathbf{r}_t and new observation \mathbf{o}_{t+1}
 Store transition $(\mathbf{o}_t, \mathbf{a}_t, \mathbf{r}_t, \mathbf{o}_{t+1})$ in \mathcal{D}
 end for
 Sample a random minibatch of M transitions from \mathcal{D}
 for each agent i **do**
 Evaluate \mathcal{L}^i and J_{PG}^i from Equations (1) and (2)
 for each other agent ($j \neq i$) **do**
 Evaluate $J_{TS}^{i,j}$ from Equations (3)
 Update actor j with $\theta^j \leftarrow \theta^j + \alpha_\theta \nabla_{\theta^j} \lambda_2 J_{TS}^{i,j}$
 end for
 Update critic with $\phi^i \leftarrow \phi^i - \alpha_\phi \nabla_{\phi^i} \mathcal{L}^i$
 Update actor i with $\theta^i \leftarrow \theta^i + \alpha_\theta \nabla_{\theta^i} (J_{PG}^i + \lambda_1 \sum_{j=1}^N J_{TS}^{i,j})$
 end for
 Update all target weights
end for

Algorithm 2 Coach

Randomly initialize N critic networks Q^i , actor networks μ^i and one coach network p^c
 Initialize N target networks $Q^{i'}$ and $\mu^{i'}$
 Initialize one replay buffer \mathcal{D}
for episode from 0 to number of episodes **do**
 Initialize random processes \mathcal{N}^i for action exploration
 Receive initial joint observation \mathbf{o}_0
 for timestep t from 0 to episode length **do**
 Select action $a_i = \mu^i(o_t^i) + \mathcal{N}_t^i$ for each agent
 Execute joint action \mathbf{a}_t and observe joint reward \mathbf{r}_t and new observation \mathbf{o}_{t+1}
 Store transition $(\mathbf{o}_t, \mathbf{a}_t, \mathbf{r}_t, \mathbf{o}_{t+1})$ in \mathcal{D}
 end for
 Sample a random minibatch of M transitions from \mathcal{D}
 for each agent i **do**
 Evaluate \mathcal{L}^i and J_{PG}^i from Equations (1) and (2)
 Update critic with $\phi^i \leftarrow \phi^i - \alpha_\phi \nabla_{\phi^i} \mathcal{L}^i$
 Update actor with $\theta^i \leftarrow \theta^i + \alpha_\theta \nabla_{\theta^i} J_{PG}^i$
 end for
 for each agent i **do**
 Evaluate J_E^i and J_{EPG}^i from Equations (7) and (6)
 Update actor with $\theta^i \leftarrow \theta^i + \alpha_\theta \nabla_{\theta^i} (\lambda_1 J_E^i + \lambda_2 J_{EPG}^i)$
 end for
 Update coach with $\psi \leftarrow \psi + \alpha_\psi \nabla_\psi \frac{1}{N} \sum_{i=1}^N (J_{EPG}^i + \lambda_3 J_E^i)$
 Update all target weights
end for

E. Hyper-parameter search

E.1. Hyper-parameter search ranges

We perform searches over the following hyper-parameters: the learning rate of the actor α_θ , the learning rate of the critic ω_ϕ relative to the actor ($\alpha_\phi = \omega_\phi * \alpha_\theta$), the target-network soft-update parameter τ and the initial scale of the exploration noise η_{noise} for the Ornstein-Uhlenbeck noise generating process (Uhlenbeck & Ornstein, 1930) as used by Lillicrap et al. (2015). When using TeamReg and CoachReg, we additionally search over the regularization weights λ_1 , λ_2 and λ_3 . The learning rate of the coach is always equal to the actor’s learning rate (i.e. $\alpha_\theta = \alpha_\psi$), motivated by their similar architectures and learning signals and in order to reduce the search space. Table 1 shows the ranges from which values for the hyper-parameters are drawn uniformly during the searches.

Table 1: Ranges for hyper-parameter search, the log base is 10

HYPER-PARAMETER	RANGE
$\log(\alpha_\theta)$	$[-8, -3]$
$\log(\omega_\phi)$	$[-2, 2]$
$\log(\tau)$	$[-3, -1]$
$\log(\lambda_1)$	$[-3, 0]$
$\log(\lambda_2)$	$[-3, 0]$
$\log(\lambda_3)$	$[-1, 1]$
η_{noise}	$[0.3, 1.8]$

E.2. Model selection

During training, a policy is evaluated on a set of 10 different episodes every 100 learning steps. At the end of the training, the model at the best evaluation iteration is saved as the best version of the policy for this training, and is re-evaluated on 100 different episodes to have a better assessment of its final performance. The performance of a hyper-parameter configuration is defined as the average performance (across seeds) of the policies learned using this set of hyper-parameter values.

E.3. Selected hyper-parameters

Tables 2, 3, 4, and 5 shows the best hyper-parameters found by the random searches for each of the environments and each of the algorithms.

Table 2: Best found hyper-parameters for the SPREAD environment

HYPER-PARAMETER	DDPG	MADDPG	MADDPG+SHARING	MADDPG+TEAMREG	MADDPG+COACHREG
α_θ	$5.3 * 10^{-5}$	$2.1 * 10^{-5}$	$9.0 * 10^{-4}$	$2.5 * 10^{-5}$	$1.2 * 10^{-5}$
ω_ϕ	53	79	0.71	42	82
τ	0.05	0.083	0.076	0.098	0.0077
λ_1	-	-	-	0.054	0.13
λ_2	-	-	-	0.29	0.24
λ_3	-	-	-	-	8.4
η_{noise}	1.0	0.5	0.7	1.2	1.6

Table 3: Best found hyper-parameters for the BOUNCE environment

HYPER-PARAMETER	DDPG	MADDPG	MADDPG+SHARING	MADDPG+TEAMREG	MADDPG+COACHREG
α_θ	$8.1 * 10^{-4}$	$3.8 * 10^{-5}$	$1.2 * 10^{-4}$	$1.3 * 10^{-5}$	$6.8 * 10^{-5}$
ω_ϕ	2.4	87	0.47	85	9.4
τ	0.089	0.016	0.06	0.055	0.02
λ_1	-	-	-	0.06	0.0066
λ_2	-	-	-	0.0026	0.23
λ_3	-	-	-	-	0.34
η_{noise}	1.2	0.9	1.2	1.0	1.1

Table 4: Best found hyper-parameters for the CHASE environment

HYPER-PARAMETER	DDPG	MADDPG	MADDPG+SHARING	MADDPG+TEAMREG	MADDPG+COACHREG
α_θ	$4.5 * 10^{-4}$	$2.0 * 10^{-4}$	$9.7 * 10^{-4}$	$1.3 * 10^{-5}$	$1.8 * 10^{-4}$
ω_ϕ	32	64	0.79	85	90
τ	0.031	0.021	0.032	0.055	0.011
λ_1	-	-	-	0.06	0.0069
λ_2	-	-	-	0.0026	0.86
λ_3	-	-	-	-	0.76
η_{noise}	0.6	1.0	1.5	1.0	1.1

Table 5: Best found hyper-parameters for the COMPROMISE environment

HYPER-PARAMETER	DDPG	MADDPG	MADDPG+SHARING	MADDPG+TEAMREG	MADDPG+COACHREG
α_θ	$6.1 * 10^{-5}$	$3.1 * 10^{-4}$	$6.2 * 10^{-4}$	$1.5 * 10^{-5}$	$3.4 * 10^{-4}$
ω_ϕ	1.7	0.94	0.58	90	29
τ	0.065	0.045	0.007	0.02	0.0037
λ_1	-	-	-	0.0013	0.65
λ_2	-	-	-	0.56	0.5
λ_3	-	-	-	-	1.3
η_{noise}	1.1	0.7	1.3	1.6	1.6

E.4. Selected hyper-parameters (ablations)

Tables 6, 7, 8, and 9 shows the best hyper-parameters found by the random searches for each of the environments and each of the ablated algorithms.

Table 6: Best found hyper-parameters for the SPREAD environment

HYPER-PARAMETER	MADDPG+AGENT MODELLING	MADDPG+POLICY MASK
α_θ	$1.3 * 10^{-5}$	$6.8 * 10^{-5}$
ω_ϕ	85	9.4
τ	0.055	0.02
λ_1	0.06	0
λ_2	0	0
λ_3	-	0
η_{noise}	1.0	1.1

Table 7: Best found hyper-parameters for the BOUNCE environment

HYPER-PARAMETER	MADDPG+AGENT MODELLING	MADDPG+POLICY MASK
α_θ	$1.3 * 10^{-5}$	$2.5 * 10^{-4}$
ω_ϕ	85	0.52
τ	0.055	0.0077
λ_1	0.06	0
λ_2	0	0
λ_3	-	0
η_{noise}	1.0	1.3

Table 8: Best found hyper-parameters for the CHASE environment

HYPER-PARAMETER	MADDPG+AGENT MODELLING	MADDPG+POLICY MASK
α_θ	$2.5 * 10^{-5}$	$6.8 * 10^{-5}$
ω_ϕ	42	9.4
τ	0.098	0.02
λ_1	0.054	0
λ_2	0	0
λ_3	-	0
η_{noise}	1.2	1.1

Table 9: Best found hyper-parameters for the COMPROMISE environment

HYPER-PARAMETER	MADDPG+AGENT MODELLING	MADDPG+POLICY MASK
α_θ	$1.2 * 10^{-4}$	$2.5 * 10^{-4}$
ω_ϕ	0.71	0.52
τ	0.0051	0.0077
λ_1	0.0075	0
λ_2	0	0
λ_3	-	0
η_{noise}	1.8	1.3

E.5. Hyper-parameter search results

The performance distributions across hyper-parameters configurations for each algorithm on each task are depicted in Figure 9 using box-and-whisker plot. It can be seen that, while most algorithms can perform reasonably well with the correct configuration, TeamReg, CoachReg as well as their ablated versions boost the performance of the third quartile, suggesting an increase in the robustness across hyper-parameter compared to the baselines.

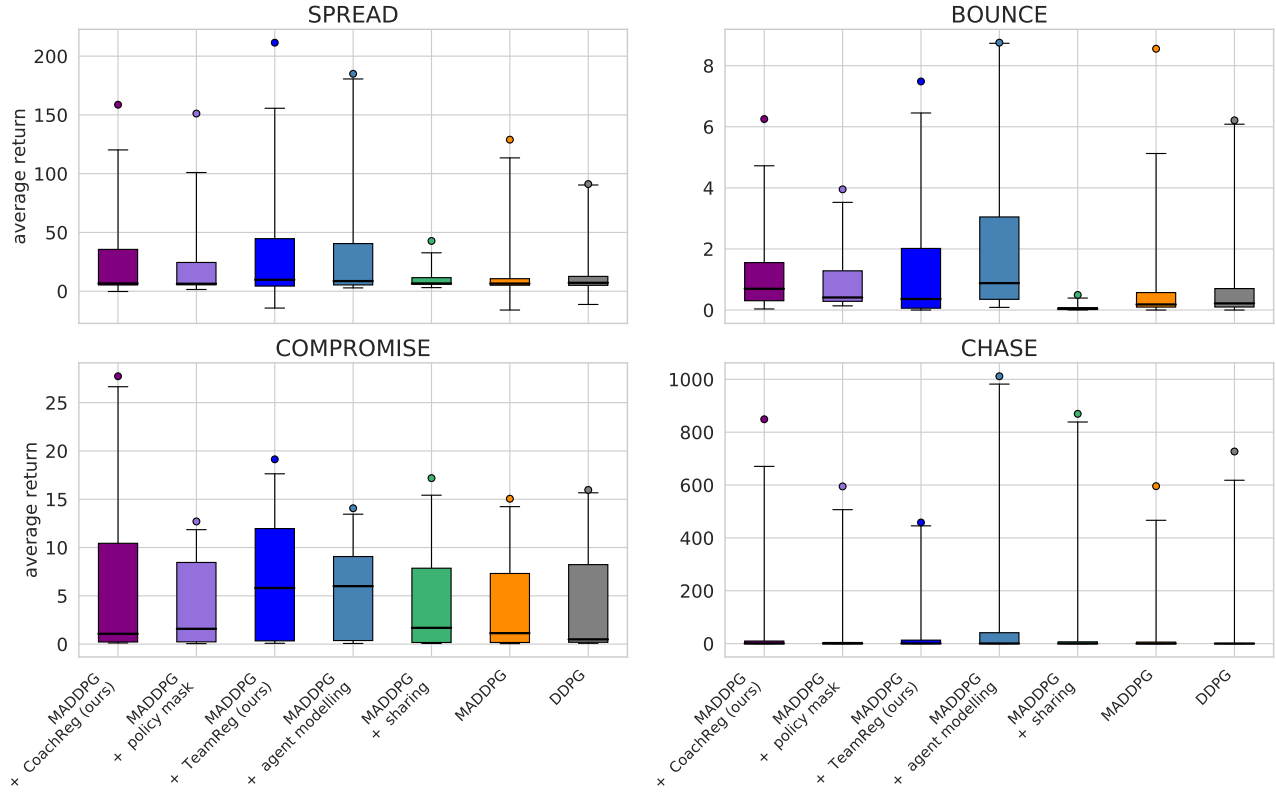


Figure 9: Hyper-parameter tuning results for all algorithms. There is one distribution per $(algorithm, environment)$ pair, each one formed of 50 data-points (hyper-parameter configuration samples). Each point represents the best model performance averaged over 100 evaluation episodes and averaged over the 3 training seeds for one sampled hyper-parameters configuration. The box-plots divide in quartiles the 49 lower-performing configurations for each distribution while the score of the best-performing configuration is highlighted above the box-plots by a single dot.

F. The effects of enforcing predictability (additional results)

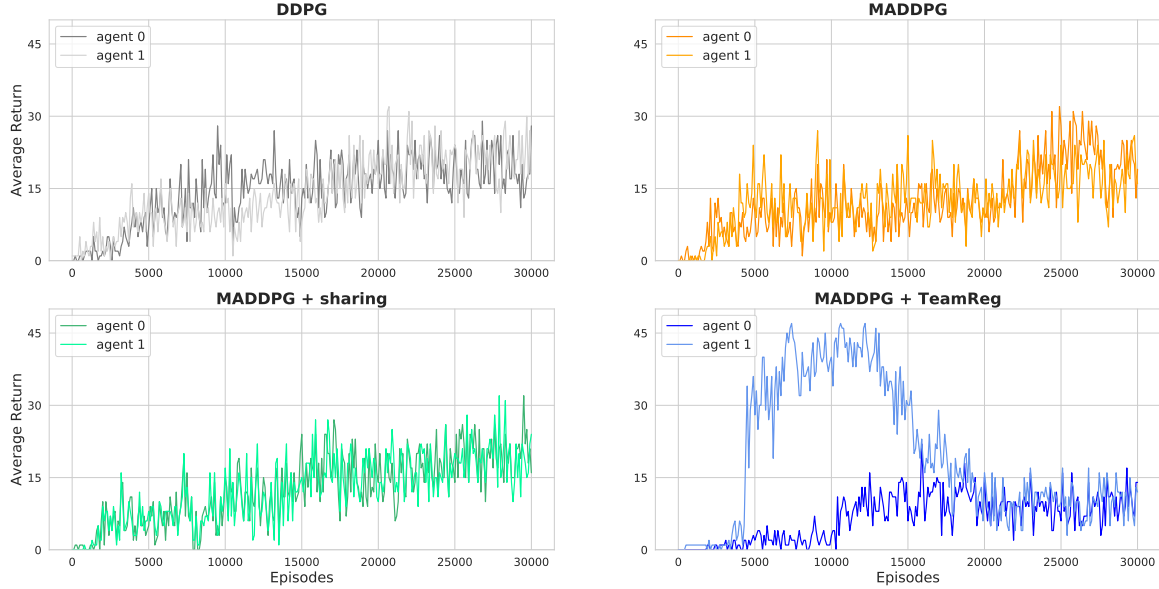


Figure 10: Learning curves for TeamReg and the three baselines on COMPROMISE. We see that while both agents remain equally performant as they improve at the task for the baseline algorithms, TeamReg tends to make one agent much stronger than the other one. This domination is optimal as long as the other agent remains docile, as the dominant agent can gather much more reward than if it had to compromise. However, when the dominated agent finally picks up the task, the dominant agent that has learned a policy that does not compromise see its return dramatically go down and the mean over agents overall then remains lower than for the baselines.

G. Analysis of sub-policy selection (additional results)

G.1. Mask densities

We depict on Figure 11 the mask distribution of each agent for each (*seed*, *environment*) experiment. Firstly, in most of the experiments, agents use at least 2 different masks. Secondly, for a given experiments, agents' distributions are very similar, suggesting that they are using the same masks in the same situations and that they are therefore synchronized. Finally, agents collapse more to using only one mask on CHASE, where they also display more dissimilarity between one another. This may explain why CHASE is the only task where CoachReg does not improve performance. Indeed, on CHASE, agents do not seem synchronized nor leveraging multiple sub-policies which are the priors to coordination behind CoachReg. In brief, we observe that CoachReg is less effective in enforcing those priors to coordination of CHASE, an environment where it does not boost nor harm performance.

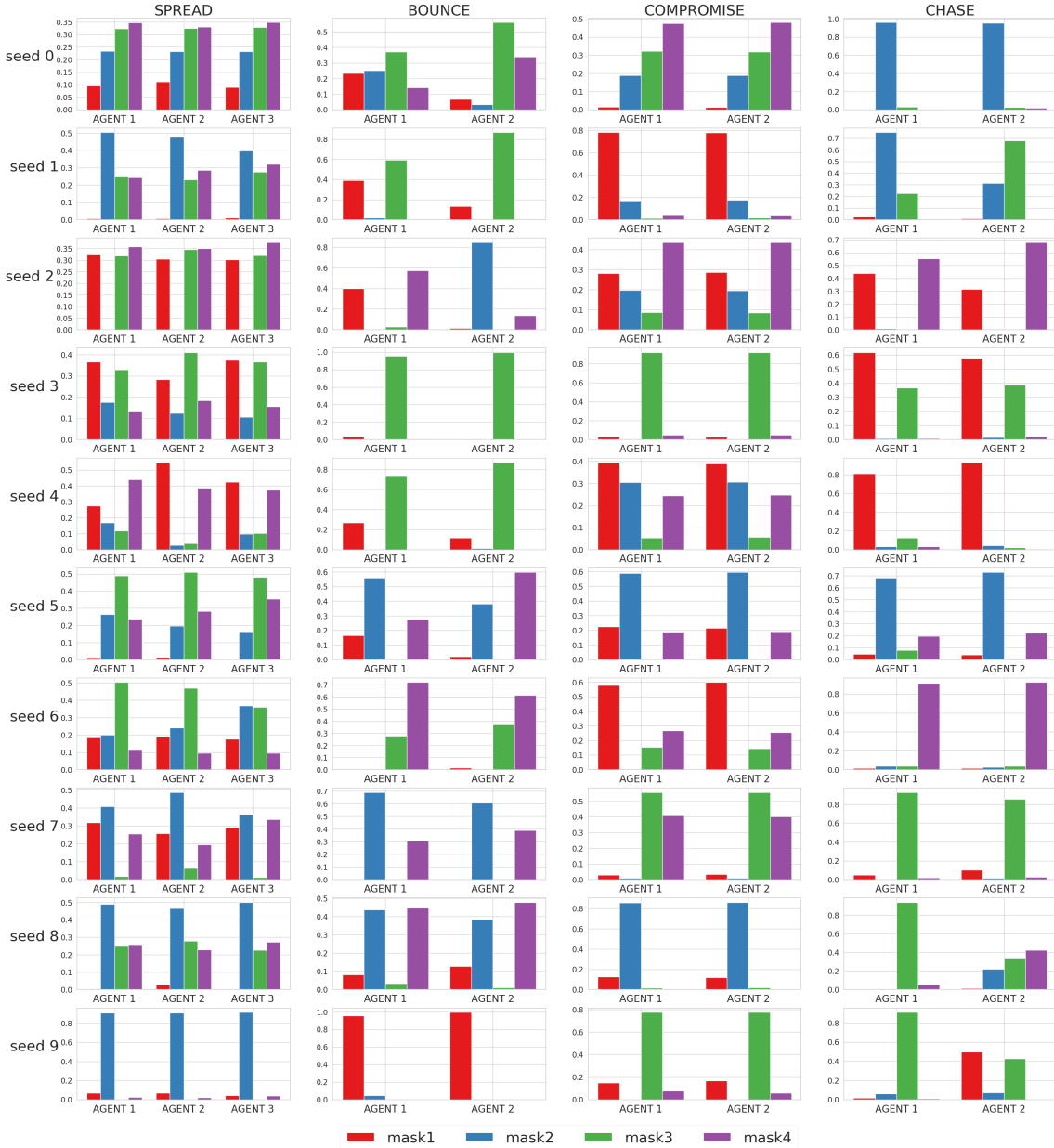


Figure 11: Agent's policy mask distributions. For each (*seed*, *environment*) we collected the masks of each agents on 100 episodes.

G.2. Episodes rollouts (see: <https://sites.google.com/view/marl-coordination/>)

On Figure 12, the agents identified two different scenarios depending on the target-ball location and use the corresponding policy mask for the whole episode. Whereas on Figure 12, the agents synchronously switch between policy masks during an episode. In both cases, the whole group selects the same mask as the one that would have been suggested by the coach.

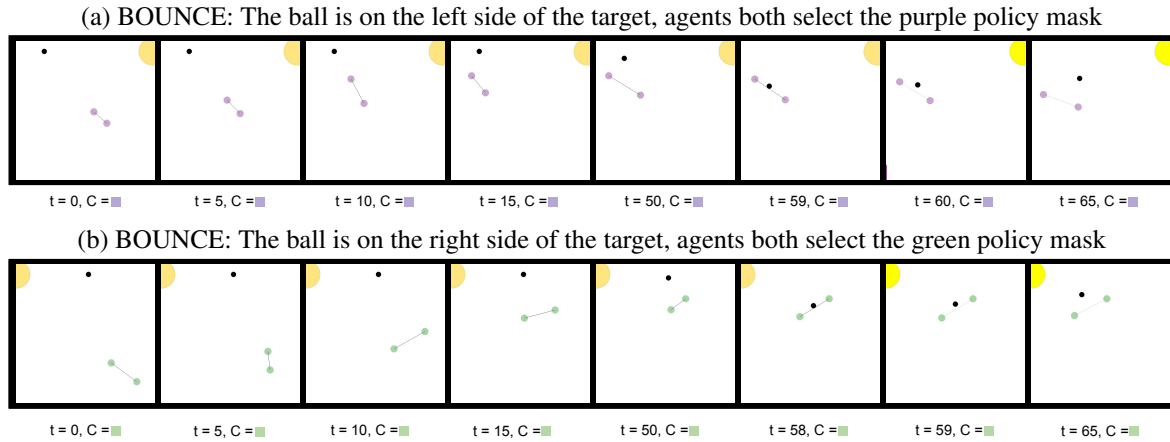


Figure 12: Visualization of two different BOUNCE evaluation episodes. Note that here, the agents' colors represent their chosen policy mask. Agents have learned to synchronously identify two distinct situations and act accordingly. The coach's masks (not used at evaluation time) are displayed with the timestep at the bottom of each frame.

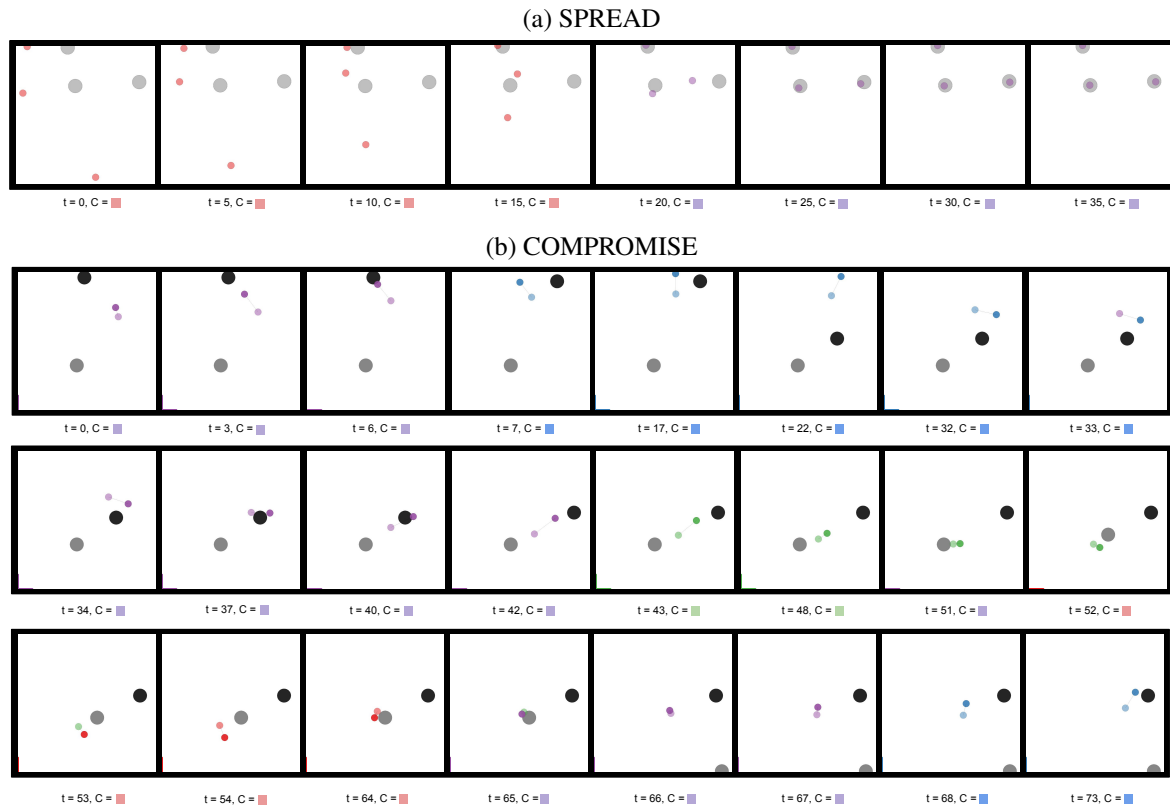


Figure 13: Visualization of sequences on two different environments. An agent's color represent its current policy mask. For informative purposes the policy mask that the coach would have produced if these situations would have happened during training is displayed next to the frame's timestep. Agents synchronously switch between the available policy masks.

G.3. Mask diversity and synchronicity (ablation)

As in Subsection G.2 we report the mean entropy of the mask distribution and the mean Hamming proximity for the ablated “MADDPG + policy mask” and compare it to the full CoachReg. With “MADDPG + policy mask” agents are not incentivized to use the same masks. Therefore, in order to assess if they synchronously change policy masks, we computed, for each agent pair, seed and environment, the Hamming proximity for every possible masks equivalence (mask 3 of agent 1 corresponds to mask 0 of agent 2, etc.) and selected the equivalence that maximised the Hamming proximity between the two sequences.

We can observe that while “MADDPG + policy mask” agents display a more diverse mask usage, their selection is less synchronized than with CoachReg. This is easily understandable as the coach will tend to reduce diversity in order to have all the agents agree on a common mask, on the other hand this agreement enables the agents to synchronize their mask selection. To this regard, it should be noted that “MADDPG + policy mask” agents are more synchronized than agents independently sampling their masks from k -CUD, suggesting that, even in the absence of the coach, agents tend to synchronize their mask selection.

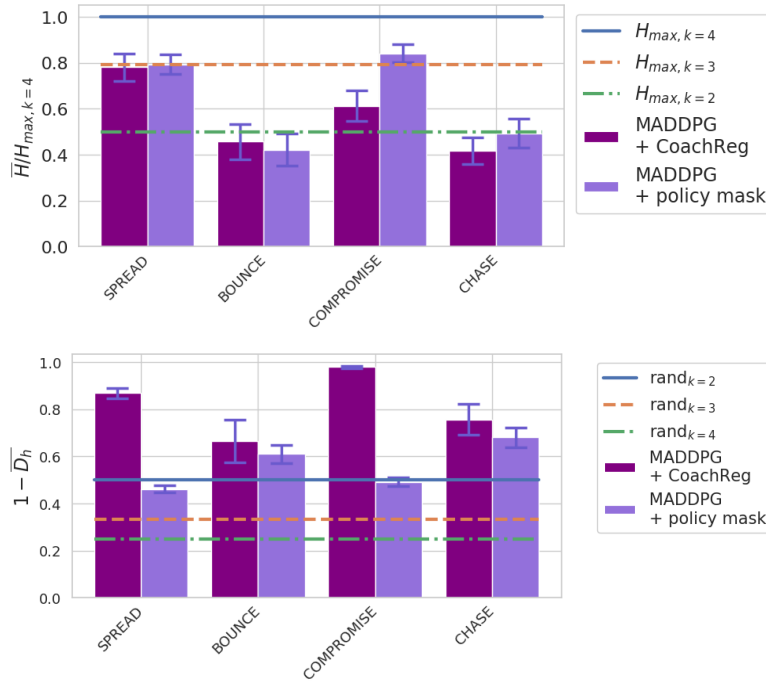


Figure 14: (Left) Entropy of the policy mask distributions for each task and method, averaged over agents and training seeds. $H_{\max, k}$ is the entropy of a k -CUD. (Right) Hamming Proximity between the policy mask sequence of each agent averaged across agent pairs and seeds. rand_k stands for agents independently sampling their masks from k -CUD. Error bars are SE across seeds.

H. Scalability with the number of agents

H.1. Complexity

In this section we discuss the increases in model complexity that our methods entail. In practice, this complexity is negligible compared to the overall complexity of the CTDE framework. To that respect, note that (1) The critics are not affected by the regularizations, so our approaches only increase complexity for the forward and backward propagation of the actor, which consists of roughly half of an agent’s computational load at training time. (2) Efficient design choices significantly impact real-world scalability and performance: we implement TeamReg by adding only additional heads to the pre-existing actor model (effectively sharing most parameters for the teammates’ action predictions with the agent’s action selection model). CoachReg consists only of an additional linear layer per agent and a unique Coach entity for the whole team (that effectively scales better than a critic since it only takes observations as inputs). As such, only a small number of additional parameters need to be learned relatively to the underlying base CTDE algorithms. For a TeamReg agent, the number of parameters of the actor increases linearly with the number of agents (additional heads) whereas the critic model grows quadratically (since the observation size themselves usually depend on the number of agents). In the limit of increasing the number of agents, the proportion of added parameters by TeamReg compared to the increase in parameters of the centralised critic vanishes to zero. On the SPREAD task for example, training 3 agents with TeamReg increases the number of parameters by about 1.25% (with similar computational complexity increase). With 100 agents, this increase is only of -2.52%. For CoachReg, the increase in an agent’s parameter is independent of the number of agent. Finally, any additional heads in TeamReg or the Coach in CoachReg are only used during training and can be safely removed at execution time, reducing the systems computational complexity to that of the base algorithm.

H.2. Robustness

We varied the number of agents present in the SPREAD task from three to six. For each algorithm we used the best performing hyper-parameter configuration from the hyper-parameter search performed on SPREAD with three agents and trained on ten different random seeds. Results are shown in Figure 15. As expected, the task becomes more complicated when the number of agents increases as the input space of the value function grows exponentially with the number of agents. Eventually, no algorithm succeeds at the task with six agents. This difficulty is likely to be exacerbated by the sparse reward setting. However, the proposed methods still outperform the baselines showing that they do not disproportionately suffer from the increased regularization pressure of additional agents.

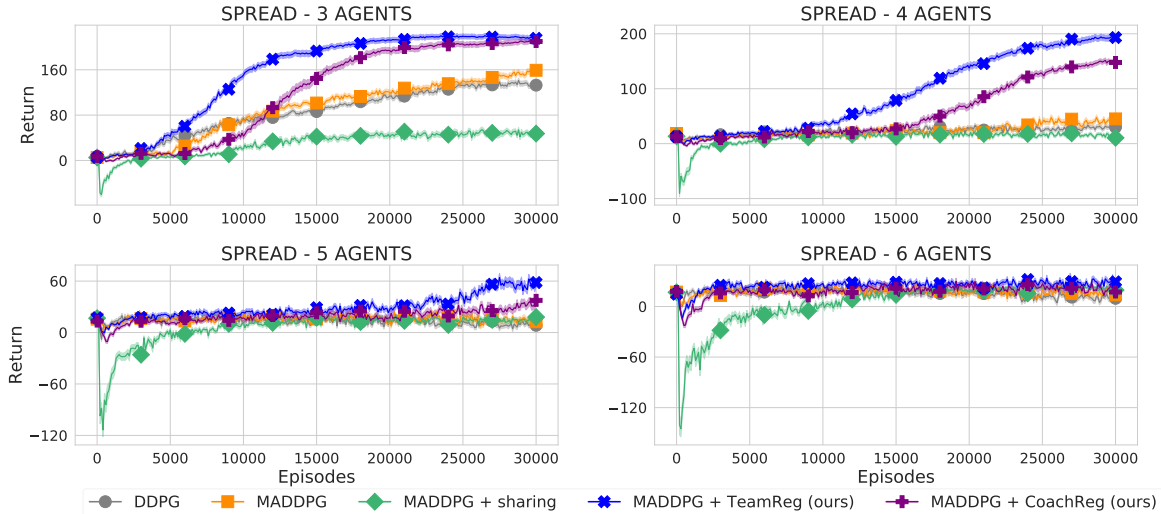


Figure 15: Learning curves (mean return over agents) for all algorithms on the SPREAD environment for varying number of agents. Solid lines are the mean and envelopes are the Standard Error (SE) across the 10 training seeds.